Geomorphology 202 (2013) 33–42

Contents lists available at ScienceDirect

Geomorphology

journal homepage: www.elsevier.com/locate/geomorph

Parameterization of rockfall source areas and magnitudes with ecological recorders: When disturbances in trees serve the calibration and validation of simulation runs

Christophe Corona [a,*], Daniel Trappmann [a], Markus Stoffel [a,b]

[a] Laboratory of Dendrogeomorphology, Institute of Geological Sciences, University of Berne, Baltzerstrasse 1+3, CH-3012 Berne, Switzerland
[b] Climatic Change and Climate Impacts, Institute for Environmental Sciences, University of Geneva, 7, chemin de Drize, CH-1227 Carouge-Geneva, Switzerland

ARTICLE INFO

Article history:
Received 4 June 2012
Received in revised form 25 September 2012
Accepted 4 February 2013
Available online 13 February 2013

Keywords:
Forest–rockfall interactions
Tree ring
Dendrogeomorphology
3D simulation model
Parameterization
Swiss Alps

ABSTRACT

On forested talus slopes which have been build up by rockfall, a strong interaction exists between the trees and the falling rocks. While the presence and density of vegetation have a profound influence on rockfall activity, the occurrence of the latter will also exert control on the presence, vitality, species composition, and age distribution of forest stands. This paper exploits the interactions between biotic (tree growth) and abiotic (rockfall) processes in a mountain forest to gather and obtain reliable input data on rockfall for the 3D process based simulation model RockyFor3D. We demonstrate that differences between the simulated and observed numbers of tree impacts can be minimized through (i) a careful definition of active source areas and (ii) a weighted distribution of block sizes as observed in the field. As a result of this field-based, optimized configuration, highly significant values can be obtained with RockyFor3D for the number of impacts per tree, so that results of the model runs can be converted with a high degree of certainty into real frequencies. The combination of the field-based dendrogeomorphic with the modeling approaches is seen as a significant advance for hazard mapping as it allows a reliable and highly-resolved spatial characterization of rockfall frequencies and a realistic representation of (past) rockfall dynamics at the slope scale.

1. Introduction

Rockfall is one of the most common geomorphic processes in mountain regions and potentially damages infrastructure or even causes loss of life (e.g. Porter and Orombelli, 1981; Erismann and Abele, 2001; Hantz et al., 2003). On forested slopes, falling rocks repeatedly interact with trees and therefore meet all the criteria to be considered as an agent of disturbance to forest dynamics (Seidl et al., 2011), since they typically disrupt forest ecosystem structure, composition and processes and ultimately cause the destruction of tree biomass (White and Pickett, 1985; Gunderson, 2000; Grime, 2001; White and Jentsch, 2001). At the forest stand level, rockfalls may (i) create patchiness or spatial heterogeneity (Veblen et al., 1994), thereby contributing largely to the existence of a wide range of ecological niches and (ii) favoring uneven-aged forests which are considered beneficial for plant diversity (Rixen et al., 2007). Through the impact of falling rocks, trees, may be uprooted, suffer from stem breakage, or decapitated if kinetic energy is transferred to the crown (Stokes, 2006). These disturbances to trees will cause immediate changes in their growth (e.g., Stoffel and Bollschweiler, 2008), thus allowing the retroactive assessment and reconstruction of past and contemporary rockfall activity (e.g., Stoffel et al., 2005a,b; Perret et al., 2006; Moya et al., 2010; Šilhán et al., 2011; Trappmann and Stoffel, 2013). Dendrogeomorphic approaches have also been demonstrated to yield in-situ information on rockfall parameters including source area, trajectories, frequency, magnitude, seasonality, or on triggers (Stoffel, 2006).

At the same time, forest structures have been shown to have physical effects on the dynamics of fallen boulders, namely on the (i) kinetic energy absorption through direct impact between a boulder and a trunk (Gsteiger, 1993; Brauner et al., 2005; Dorren et al., 2005; Stokes et al., 2005; Dorren et al., 2007; Lundström et al., 2007, 2009); (ii) energy dissipation (i.e. kinetic energy absorption) of rockfalls by coppice structures through the interaction between a rock and shrub vegetation (Ciabocco et al., 2009); as well as on the (iii) the positive effect of forest vegetation on geotechnical soil characteristics (Pfeiffer, 1989). Forests can thus act as protective shields for downslope reaches and prevent rockfall from affecting inhabited areas.

At locations where hazardous rockfall events have occurred in the past, 3D rockfall simulations are often used to determine runout distances, energies, preferential paths and bounce heights of rockfalls (Dorren, 2003), with some of these models explicitly simulating collisions with trees. The primary goal of performing model runs on forested slopes is for a realistic hazard assessment and secondly for a quantification of the role of forests in protecting human lives and their assests (Dorren et al., 2005). Crucial parameters for such an approach are the identification of source areas, determination of fall tracks, and the calculation of rockfall velocity (which depends on

* Corresponding author.
E-mail address: christophe.corona@dendrolab.ch (C. Corona).

0169-555X/$ – see front matter
http://dx.doi.org/10.1016/j.geomorph.2013.02.001

the interaction of rocks and boulders with the forest stand which will in turn determine runout distance (Dorren, 2003). Reliable model data can, however, only be obtained if a detailed database exists on the position of source areas, potential rock sizes, and slope properties. Such field information is crucial for a realistic calibration of model parameters, for verification of model results, and for the reduction of differences between model output and reality.

Model verification can be done through the study of orthophotos, field visits, and the analysis of archival records (Dorren and Berger, 2006). Yet, as a result of the sudden occurrence and unpredictable nature of rockfalls, such data are only rarely available. Real-time observations of rockfalls do not normally exist either since they are very time consuming and only available (if at all) for small sites and for a short period of time (Luckman, 1976; Douglas, 1980; Gardner, 1980; Matsuoka and Sakai, 1999). The perusal of archival data remains usually scarce and fragmentary as well (e.g. Dussauge-Peisser et al., 2002), and records usually contain information on events that caused fatalities or destruction of human assets, but will lack data on small-scale events and activity in less-densely inhabited areas (Stoffel, 2006).

This study therefore aims at (i) improving available data on rockfalls, (ii) enhancing delineation of source area and (iii) at better defining magnitude and frequency of rockfalls by calibrating the simulation model RockyFor3D with a dense set of dendrogeomorphic data. We also illustrate how differences between modeling and dendrogeomorphic reconstructions can be minimized through the use of a block size distribution in the model which is similar to the one measured in the field.

2. Study site

The east-facing Raaftgarte slope analyzed in this study is located in the Saas Valley, southern Swiss Alps (46°12′36″ N., 7°53′08″ E.), just above the main road (2,500 vehicles per day on average) connecting Stalden to Saas Fee (Fig. 1A, B). Rockfall is frequent at the site and fragments are normally detached from several release zones within a roughly 340-m high rock face (1140–1480 m asl). In the adjacent transit area (1020–1140 m asl, mean slope of 38°), Quaternary deposits are dominated by a mosaic of vegetated surfaces, intermittent scree slope deposits and an open forest stand composed of Silver birch (*Betula pendula* Roth) and European larch (*Larix decidua* Mill.) trees (Fig. 2A, B).

Bedrock in the release areas is composed of tectonized, fine grained gneisses (Bearth, 1978) belonging to penninic crystalline units. A major rockfall event (80 m^3) has been reported for the site on 14 November 2002, when a portion of the lower release area collapsed as a result of repeated freeze-thaw cycles of meltwater in the joint system. This event resulted in the partial destruction of the forest stand and road at and next to the southernmost segment of the study site. To protect the main road from the hazardous impacts of rockfalls, several rows of flexible rockfall nets have been installed in the northern part of the slope in 1990. The volume of rock fragments observed in the nets does not usually exceed 0.1 m^3 (99th percentile), and the largest individual block observed in the field has 2.4 m^3.

3. Material and methods

3.1. The dendrogeomorphic approach

Based on the geomorphic mapping, rockfall can be considered the only geomorphic process damaging trees at the study site. As a result, trees were selected randomly on the slope with special attention being paid to a regular distribution of sampled trees across the study perimeter. Coordinates of trees were recorded with a compass, inclinometer and measuring tape and imported into a GIS system.

Since the period during which rockfall scars remain visible on the tree bark primarily depends on the tree species (Stoffel and Perret, 2006), different strategies were applied to derive the number of rockfall events at the study site. The first species analyzed, *L. decidua*, is known to mask injuries efficiently, so that event histories at the level of individual trees were reconstructed with increment cores (max. 40 × 0.5 cm) and through the presence of tangential rows of resin ducts (TRD; Bannan, 1936; Stoffel, 2008) being formed next to and at some distance of the impact scar (Schneuwly, 2009; Schneuwly et al., 2009). In the case of *L. decidua*, sampling positions on the stem were therefore adapted to observed bounce heights which remain usually below 2 m at the study site. Increment cores were consequently extracted at 0.5, 1.0, and 1.5 m in case that signs of past injuries were not visible on the stem surface. One additional core was extracted on the undisturbed downslope side so as to determine tree age. In the case of visible scars, additional cores were extracted as close to the injury as possible following Schneuwly et al. (2009).

In the case of *B. pendula*, its non-peeling bark structure will leave mechanical impacts visible on the trunk surface over decades ., and past rockfall activity was assessed by simply counting visible scars on the stem surface (Trappmann and Stoffel, 2013). In addition, one increment core was extracted on the undisturbed downslope side of the tree as close to ground level as possible so as to determine tree age.

All cores were processed with fine grained sanding paper and tree rings were analyzed under a LINTAB positioning table following standard procedures as described in Stoffel and Bollschweiler (2008). As the accurate dating of events was not the primary goal of this study, we disclaimed the cross-dating procedure and derived tree age and number of impacts without measuring tree-ring widths. Events in *L. decidua* were dated through the identification of growth disturbances (GD) related to mechanical disturbances (Stoffel and Bollschweiler, 2008; Stoffel et al., 2010), but primarily through the presence of TRD and callus tissue (Stoffel and Hitz, 2008).

Return periods of rockfall were calculated for each individual tree by dividing its age with the number of impacts. As impacts in case of *L. decidua* were identified within a timeframe given by the tree-ring series, the longest record of a given tree was considered to represent its age. For *B. pendula*, in contrast, injuries were assumed to stay visible on the stem surface over the whole lifespan of the tree, and the real age (germination age) was used in the reconstruction. Rings missing from the inner end of the increment core to the pith were added using a transparent template of concentric rings. In addition, missing rings originating from sampling height above ground level were added following the approach described in Bollschweiler et al. (2008).

3.2. The Rockyfor3d modeling approach

In a subsequent step, rockfalls at Raaftgarte were simulated using RockyFor3D (Dorren, 2012), a probabilistic process-based rockfall trajectory model that combines physically-based, deterministic algorithms with stochastic approaches to simulate rockfall in its three dimensions. The model consists of three main modules.

The first module calculates rockfall trajectories by calculating sequences of classical parabolic free fall through the air and rebounds on the slope surface. During each rebound, the model allows the block to deviate from its direction before rebound toward the direction of the aspect of the raster cell in which the block rebounds. Hence, the model produces diverging rockfall trajectories. The second main module calculates energy loss due to impacts against single trees. The exact position of a falling rock and its current energy are modeled. If an impact against a tree takes place, part of the rock energy is dissipated as a function of the relative position between rock and tree center and the stem diameter of the corresponding tree. After a tree impact, the trajectory of a rock can be deviated laterally up to

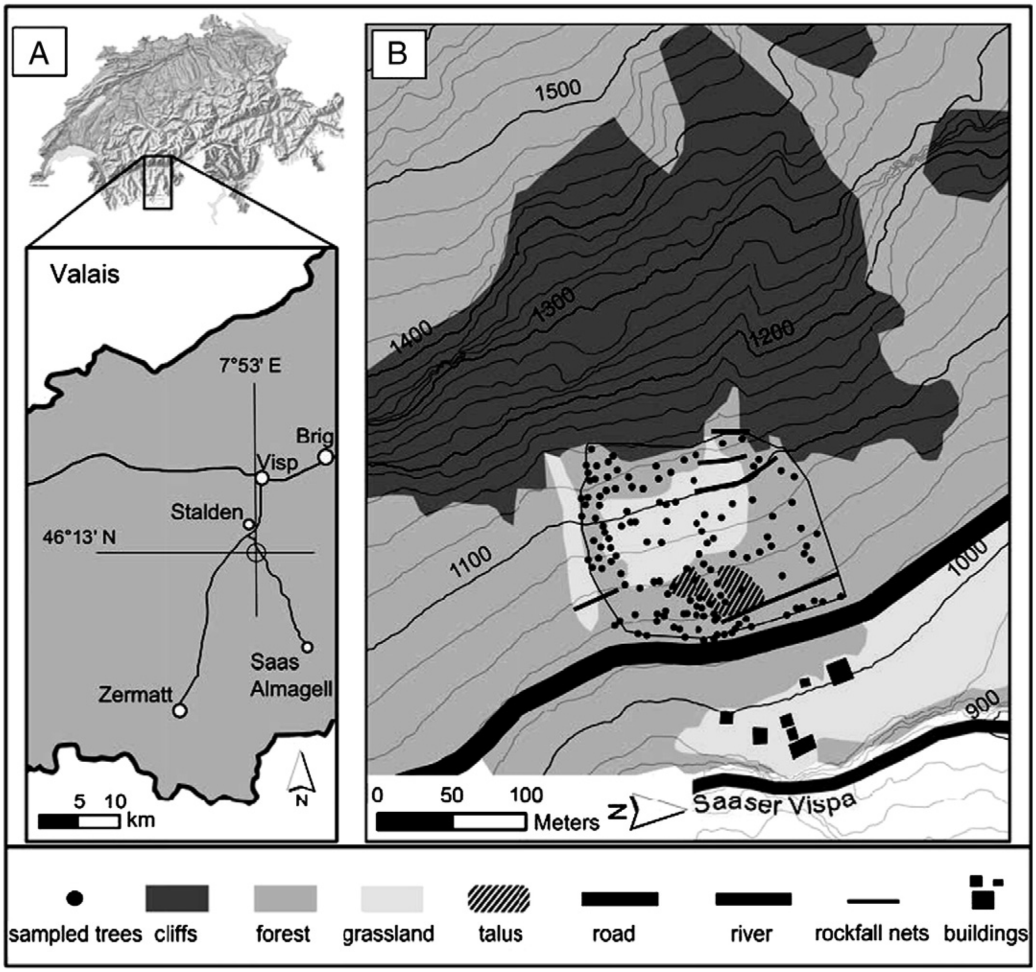

Fig. 1. (A) The Raaftgarte study site is located in the Saas Valley, southern Swiss Alps. (B). Sketch map of the study site with the position of the 133 trees used for dendrogeomorphic analyses.

76° from its fall direction before the tree impact. The third module calculates the velocity of the falling rock after a rebound on the slope surface (for details see Dorren, 2012).

3.3. Model input data

The required model input data consist of a set of raster maps which describe the (1) Digital Elevation Model (DEM), (2) rockfall source cells including rock density, dimensions and shape, (3) number of trees per cell, (4) distribution of trees in each cell, (5) wood type per cell (broadleaved or coniferous), (6) plasticity of the surface material per cell and (7) roughness of the slope surface per cell.

At Raaftgarte, a high resolution DEM (2.5×2.5 m) was produced through the interpolation (Ordinary Kriging) of LIDAR (LIght Detection And Ranging laser scanning) point data with an average of 12 points per raster cell.

Thereafter, potential rockfall source areas were mapped, integrated into a Geographical Information System (GIS) and converted to raster

Fig. 2. (A) Lateral view of the rockfall slope (mean slope angle 38°) (B).View from the bottom of the study site to the cliffs where rockfall is released.

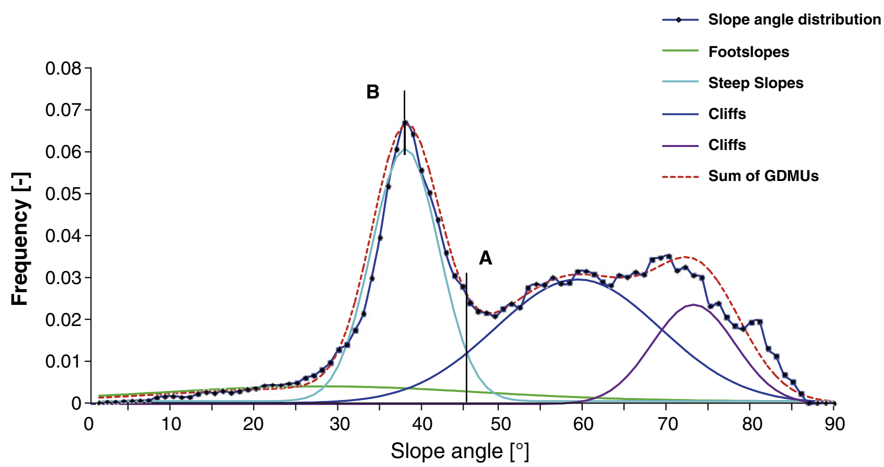

Fig. 3. Normal distribution of slope angles at the study site as extracted from a 2.5 m-DEM using the HistoFit routine. Here, slopes are decomposed in four normal distributions. "A" indicates the threshold slope angle above which the slopes belong predominantly to the cliffs and are therefore considered as potential rockfall source area for simulation S2. "B" indicates the mode of the "steep slopes" morphological unit.

maps. Three different approaches were used for the mapping of source areas: In a first approach, thresholds for mean slope gradients were defined following Toppe (1987) and van Dijke and van Westen (1990). In a second approach, potential rockfall source areas were mapped based on the slope angle distribution deduced from high resolution DEM (Loye et al., 2009). In a third approach, rockfall source areas were determined based on expert mapping of cliff faces from topographic (Meissl, 1998), geomorphic, and geologic (van Dijke and van Westen, 1990) maps.

To test the potential of dendrogeomorphic data in delineating optimal source areas, three sets of data were produced. For simulation 1 (S1), potential rockfall source cells were defined with a mean slope gradient >65°. This threshold corresponds to the transformation from a falling to a bouncing mode of motion for blocks (Dorren, 2003). Below this threshold, the rock collides with the slope surface after free falling, and 75–86% of the energy gained in the initial fall will be lost during first impact (Dorren, 2003).

For S1, source cells were systematically extracted from the slope map derived from the DEM using ArcGIS software. For simulation 2 (S2), the slope angle distribution was decomposed in several Gaussian distributions which can be considered characteristic of morphological units (such as rock cliffs, steep slopes, foot slopes, and plains) using the HistoFit routine (Loye et al., 2009, Fig. 3). The terrain is considered a potential rockfall source if its slope angle exceeds an angle threshold, which is in turn defined where the Gaussian distribution of the morphological unit «rock cliff» becomes dominant over the «steep slope» unit. According to this analysis, the threshold slope angle for source areas was fixed to 47° (Fig. 3). Finally, for simulations 3–7 (S3–S7), active source areas of rockfall were determined from geomorphic and geologic maps and based on field observations.

In the transit area, the characteristics of the forest stand (position and diameters of trees and tree species) were determined by field measurements and data transferred into the GIS system. Similar characteristics were used for all the simulations. The energy dissipation capacity of the surface material and the roughness of the slope surface were derived from polygons representing homogeneous terrain units as mapped in the field and converted into a raster map. The energy dissipation capacity of the surface material is represented by a normal coefficient of restitution (rn). The roughness of the slope surface, in combination with the rock radius and the depth of the impact crater during a rebound, was entered in an automatic calculation of the tangential coefficient of restitution (rt; Dorren et al., 2006). In the model, both coefficients of restitution are determined by the composition and size of the material covering the surface and the radius of the falling rock itself.

3.4. Simulation set-up

For all seven simulations performed in this study, the initial fall height of rocks in the rockfall start cells was set to 2 m. As a consequence, cliff faces from which rockfalls may start were at least 2 m high.

Based on a sensitivity test of the model, repeating simulations 100 times from each source cell using the Monte Carlo method (Lewis and Orav, 1989; Mowrer, 1997) has been shown to produce sufficiently stable results. This means that from a cliff consisting of 200 rockfall source cells, 20,000 rocks were simulated and different trajectories and velocities obtained. This number of repetitions was considered an acceptable tradeoff between computation time and stability of results and was therefore used for all the simulations.

To account for the varying size of falling rocks and boulders at the site, we simulated varying block sizes. For S1, S2 and S3, where the aim was to delineate optimal source areas, the mean diameter of falling blocks was set to 0.18 m. This value corresponds to the mean diameter of rocks deposited in the rockfall nets since 1990 (i.e. the mean size of blocks which have been deposited during the past 20 yr). Random rock volume variations in the start cells were set to ±50%.

The diameter size distribution of rocks and boulders within the nets is similar to a Gaussian distribution (Fig. 4), but the RockyFor 3D code does not allow to model such a distribution. However, in order to take account of the distribution, four additional simulations (S4, S5, S6, S7) were produced with block diameters of 0.18 m (mean diameter of

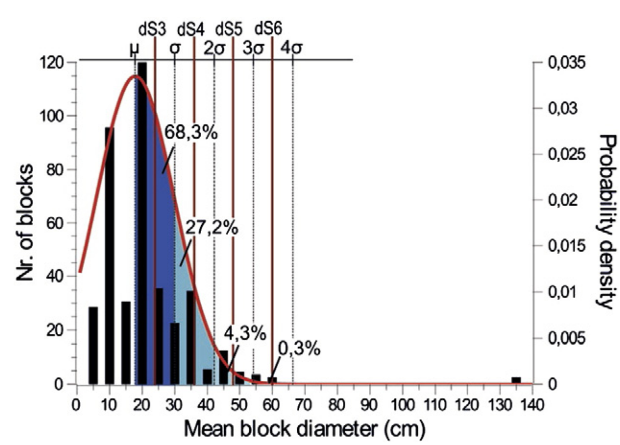

Fig. 4. Normal probability distribution derived from the histogram of rock diameters observed in the nets.

Table 1
Characteristics of the trees sampled.

Species	Sampled trees	Cores	Mean age/yrs (St Dev)	Reconstructed events
Larix decidua (cores)	40	136	56 (24)	107
Larix decidua (count)	1	1	56 (–)	16
Betula pendula	83	83	51 (23)	579
Corylus avellana L.	2	2	41 (3)	8
Fraxinus sp.	6	6	39 (28)	26
Sorbus aria (L.) Crantz	1	1	54 (–)	1
Total	133	229	52 (23)	737

blocks in the rockfall nets, ±50%), 0.30 m (mean + 1sd, ±50%), 0.42 m (mean + 2sd, ±50%), and 0.54 m (mean + 3sd, ±50%) for S4, S5, S6, and S7, respectively. The nature of the Gaussian distribution gives a probability of 0.683 for a block diameter being in the range used in S4 (0.18–0.3 m); 0.272 for a block diameter being in the range of S5 (0.3–0.42 m); 0.042 for a block diameter being in the range of S6 (0.42–0.54 m); 0.003 for a diameter block diameter being in the range of S7 (>0.66 m). A composite simulation S8 was therefore produced as the weighted sum of simulations S4–S7 and taking account of these probabilities.

3.5. Quantification of model accuracy

Results from the simulation runs and the dendrogeomorphic analysis were compared on the basis of the spatial distribution of rockfall impacts on trees, as it is an indicator for the spatial distribution of rockfall trajectories. However, and as a result of the repeating number of simulations, the total number of simulated impacts on trees greatly exceeds the number of GD obtained with dendrogeomorphic techniques. A normalized number of simulated impacts *Nnorm* was therefore calculated for each tree (i) to render both techniques comparable:

$$Nnorm_i = \frac{(Nsimul_i * N_{GD})}{Ntotsimul}$$

where *Nsimul* represents the number of impacts simulated at tree i, N_{GD} the total number of growth disturbances (GD) obtained with dendrogeomorphic techniques ($N_{GD} = 737$) and *Ntotsimul* the total number of simulated impacts.

In a subsequent step, mean errors (*ME*) between the predicted and the observed number of impacts were calculated for each tree following:

$$ME_i = Nnorm_i - GD_i$$

where *Nnorm* is the normalized predicted (i.e. simulated) number of rock impacts; and *GD* the observed number of growth disturbances at tree i. In order to compare simulations, the Mean Absolute Error (*MAE*) was computed, at the slope scale, as follows:

$$MAE = \frac{1}{n}\sum_{i=1}^{n} |ME_i|$$

where n is the total number of trees in dendrogeomorphic analysis ($n = 233$) and ME_i, the mean error computed at tree i.

4. Results

4.1. Growth disturbances in trees

A total of 133 trees (69% *B. pendula*, 31% *L. decidua*) with obvious signs of rockfall impacts were investigated at Raaftgarte (Table 1). The mean age of the sampled trees is 52 ± 23 yr. Analysis of the increment cores sampled from *L. decidua* resulted in 107 reconstructed rockfall events since AD 1905 whereas the systematic observation of rockfall scars on the stem surface of *B. pendula* yielded 630 rockfall impacts (737 rockfall impacts; mean: 5.5 ± 5.4 GD, max: 31 GD, min 1 GD). The spatial distribution of trees and their absolute number of scars is given in Fig. 5 and points to a large activity close to the apex of the scree slope and a decrease in activity further downslope. Activity seems to be most important (~10 impacts per tree) near the cliff in the north-westernmost segment of the slope, but this increase in activity is probably reflective of the large rockfall event of November 2002. Return periods of rockfall at the tree level at the study site vary between 1.3 and 95 yr.

4.2. Model accuracy

Simulations S1, S2 and S3 aimed at calibrating rockfall source cell areas. In total, 395,700, 1,134,300 and 59,300 rockfalls were simulated for S1, S2 and S3, respectively (Table 2). These rockfalls caused 26,479, 88,282 and 6,402 impacts to the 133 trees sampled for dendrogeomorphic analyses. After normalization, the maximum numbers of simulated impacts were 14.2, 17.6 and 13.2 hits per tree for S1 and S2 and S3 respectively, with return periods varying between 2.3 and 78.6 yr for S1, 1.5 and 67 yr for S2, and 1.9 to 99.9 yr for S3.

Regarding the overall distribution of rock impacts per tree, the number of tree hits is largest close to the apex of the scree slope and where rockfall source areas are closest (Figs. 6A, 7A, 8A). This number again decreases downslope, and closer to the road. The ME maps (Figs. 6B, 7B, 8B) evidence an important underestimation of

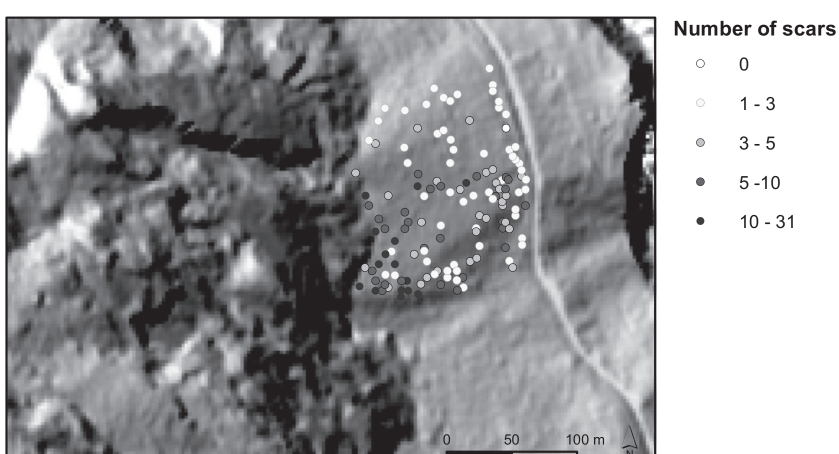

Fig. 5. Spatial distribution of observed (absolute numbers of) scars. The largest activity is observed on the north-westernmost part of the slope, the lowest activity in its northern part and at the bottom of the study site.

Table 2
Simulations set-up and Mean Absolute Errors (MAE) computed between observed and simulated number of tree impacts.

	S1	S2	S3	S4	S5	S6	S7
Rock diameter (m)	0.18	0.18	0.18	0.18	0.3	0.42	0.54
Nb of source cells	3957	11343	593	593	593	593	593
Nb of rockfalls	395,700	1,134,300	59,300	59,300	59,300	59,300	59,300
Number of impacts	26,479	88,282	6402	6402	7258	7478	7699
Total (maximal) Nb of impacts on trees after normalization	737 (max:14.2)	737 (max:17.6)	737 (max: 13.2)	737 (max: 13.2)	737 (max: 16)	737 (max: 14.5)	737 (max: 18.1)
Weight	1	1	1	0.683	0.272	0.042	0.003
Mean Absolute Error (MAE)	4	4.5	3.7	Composite simulation S8: 3.2			

the observed number of impacts in the south-easternmost part of the study site at Raaftgarte. Conversely, the number of impacts is slightly overestimated in the central part of the slope. The MAE associated to S1, S2, and S3 are 4, 4.5 and 3.7, respectively. Comparisons of the maps illustrated in Figs. 6B, 7B, and 8B demonstrate that decreasing MAE in S3 compared to S1 and S2 is in fact related to a slight reduction of ME over the entire slope.

In simulation S8, a composite of simulations S4–S7, the probability (1990–2011) for a given block size to reach the study site was taken into account by using the Gaussian distribution of blocks as deposited in the rockfall nets since 1990 and by including the weighted and normalized contributions of S4–S7 (i.e. simulations with different block sizes) according to their presence as observed in the field. In the composite model, where both the number and block sizes should best represent real rockfall activity, a maximum number of 16.5 impacts per tree is obtained (Fig. 9A) with a MAE of 3.2. This decrease in MAE as compared to results obtained with S1–S3 is especially related to ME reductions in trees located in the south-easternmost part of the slope (Fig. 9B). Interestingly, the MAE becomes comparable for both *L. decidua* (3.1) and *B. pendula* (3.3) when this optimal configuration is being used. The MAE in *L. decidua* mainly (85%) represents an overestimation of the observed number of GD (for 31 out of the 41 sampled trees). Conversely, the MAE in *B. pendula* more frequently reflects underestimation (43 trees, 75%) rather than overestimation (49 trees, 25%) of the observed number of GD.

5. Discussion

5.1. Calibration of the RockyFor3D model

Trees and rockfalls interact and depend on each other in complex ways (Marston, 2010; Seidl et al., 2011). Rockfall processes exert

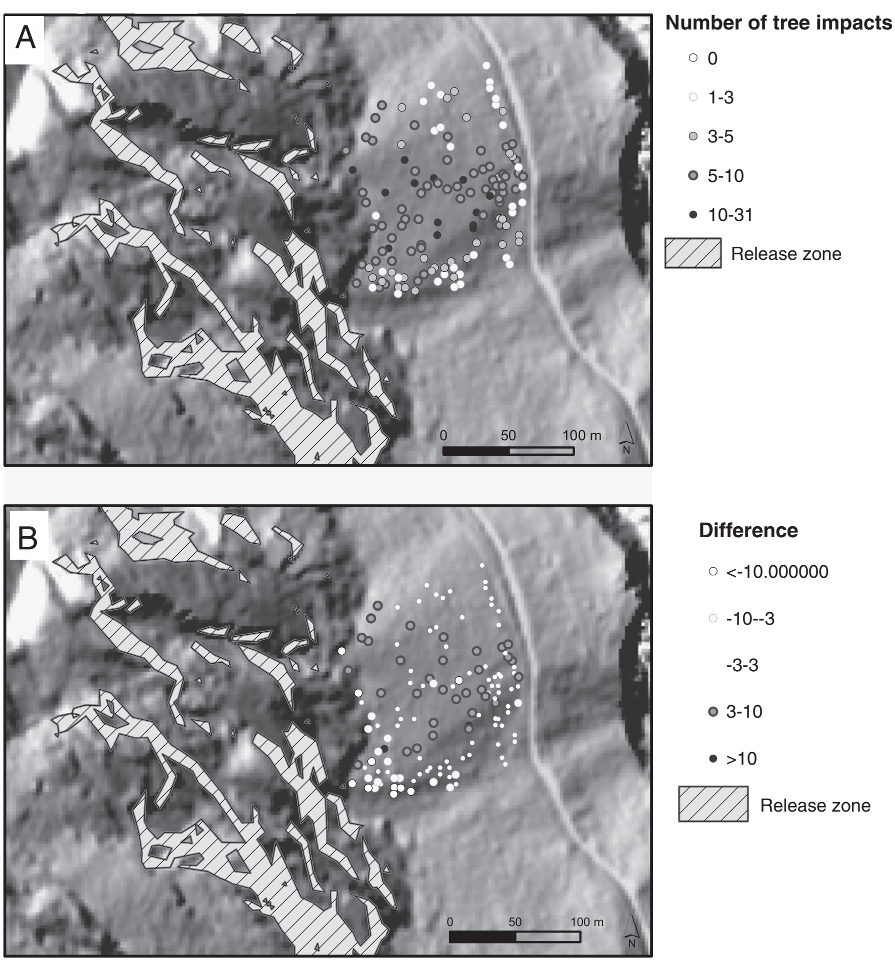

Fig. 6. (A) Spatial distribution of the normalized number of tree impacts for simulation S1 (slope in release areas >65°) and (B) differences between the simulated and observed number of rock impacts.

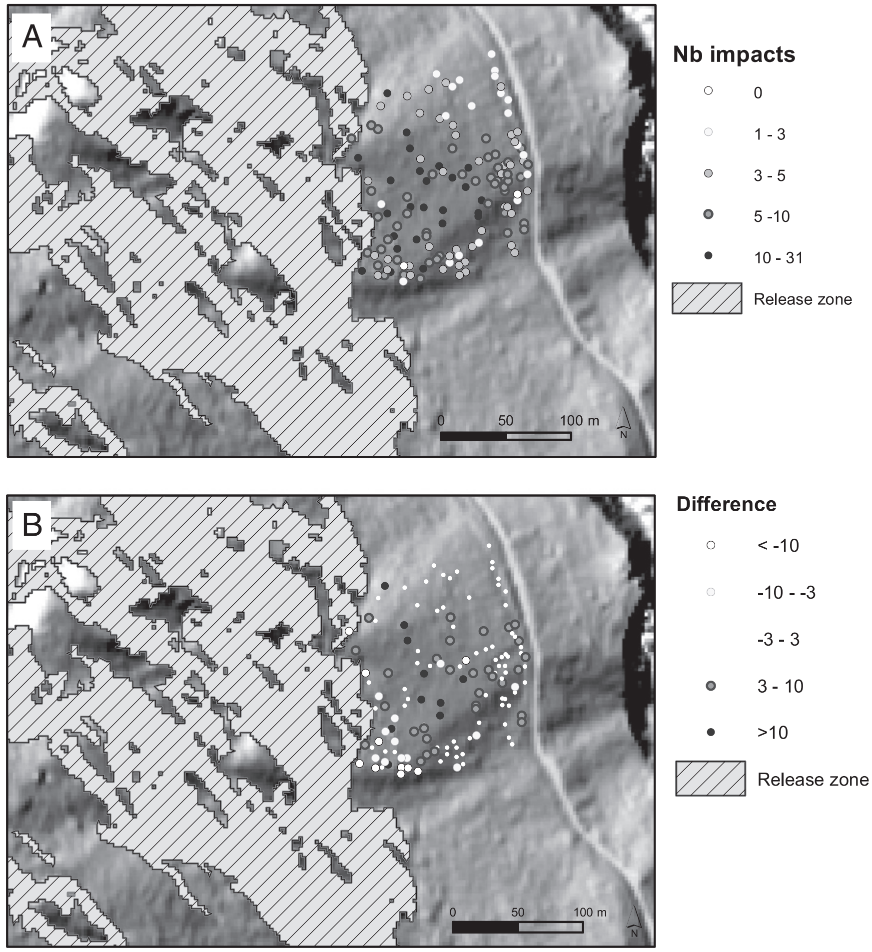

Fig. 7. (A) Spatial distribution of the normalized number of tree impacts computed with simulation S2 (i.e. slope in release areas is >47°) and (B) differences between the simulated and observed number of rock impacts on trees.

control on the presence, vitality and age distribution of forest stands, and the presence and density of trees also has a profound influence on rockfall processes. These interactions between vegetation and gravitational processes can be simulated in 3D simulation models as the energy loss of falling rocks due to collisions with trees and as the deviation of rocks from the principal fall line following tree impacts (Dorren et al., 2006). Vegetation affected but not killed by rockfalls will integrate the effects of such disturbances with specific and immediate growth reactions in their tree-ring record (e.g., Stoffel and Bollschweiler, 2008).

In this study, we combined the dendrogeomorphic and the modeling approaches. Rockfall frequencies derived from the dendrogeomorphic analysis of 133 trees were used to (i) better delineate the source areas and the magnitude–frequency of rockfalls produced by the latter in the 3D rockfall simulation model RockyFor3D as well as to (ii) test its capability to accurately predict rockfall patterns on a forested slope. Data on 737 rockfalls visible on stem surface of *B. pendula* or conserved in the form of growth anomalies in the tree-ring record of *L. decidua* were used to derive rockfall activity at Raaftgarte (Swiss Alps). The information contained in the tree-ring record was of utmost help for the accurate delineation of rockfall source areas. Our study suggests that the closest match between dendrogeomorphic and simulated distributions of tree impacts is obtained using rockfall source areas based on direct observations in the field and geologic advisory opinions rather than from mean slope gradients (>60°). Data also confirms that model output improves considerably if rockfall source areas (such as small cliff faces) and active sources of rockfall are identified manually rather than retrieved using a mean slope gradient threshold value. The accurate delineation of rockfall source areas has in fact been demonstrated to be decisive for a better prediction of rockfall trajectories and, consequently, impacts with trees. We are well aware that, as a result of the complex terrain features and the presence of a 340-m high cliff, the delineations presented will remain an approximation to reality. Nonetheless, we were able to obtain a more precise assessment of rockfall sources through the use of iterative processes and the systematic computation of the MAE.

After the calibration of the rockfall source areas, the comparison of the spatial distribution of rockfall activity derived from tree-ring analysis with that obtained with the modeling approach showed an improved correspondence. In particular, the decreasing number of tree impacts in the downslope direction was very accurately and correctly reproduced by the model. Our results further demonstrate that the weighting of the block sizes according to the probabilities given by a Gaussian distribution, as observed in the rockfall nets (1990–2011), will ultimately result in a significant decrease of the MAE and in a better estimation of rock–tree interactions. In that sense, our study also confirms that – in addition to a good record of past events – a detailed database on sizes of rocks and boulders as present on the site is required to retrieve reliable data from GIS-based modeling approaches (Schneuwly, 2009). In that sense, rockfall nets are certainly valuable sources of information for the evaluation of rock sizes representative of activity over the past decades. The distribution of block in nets can be considered homogeneous, which is in contrast to talus slope deposits where large boulders tend to travel further

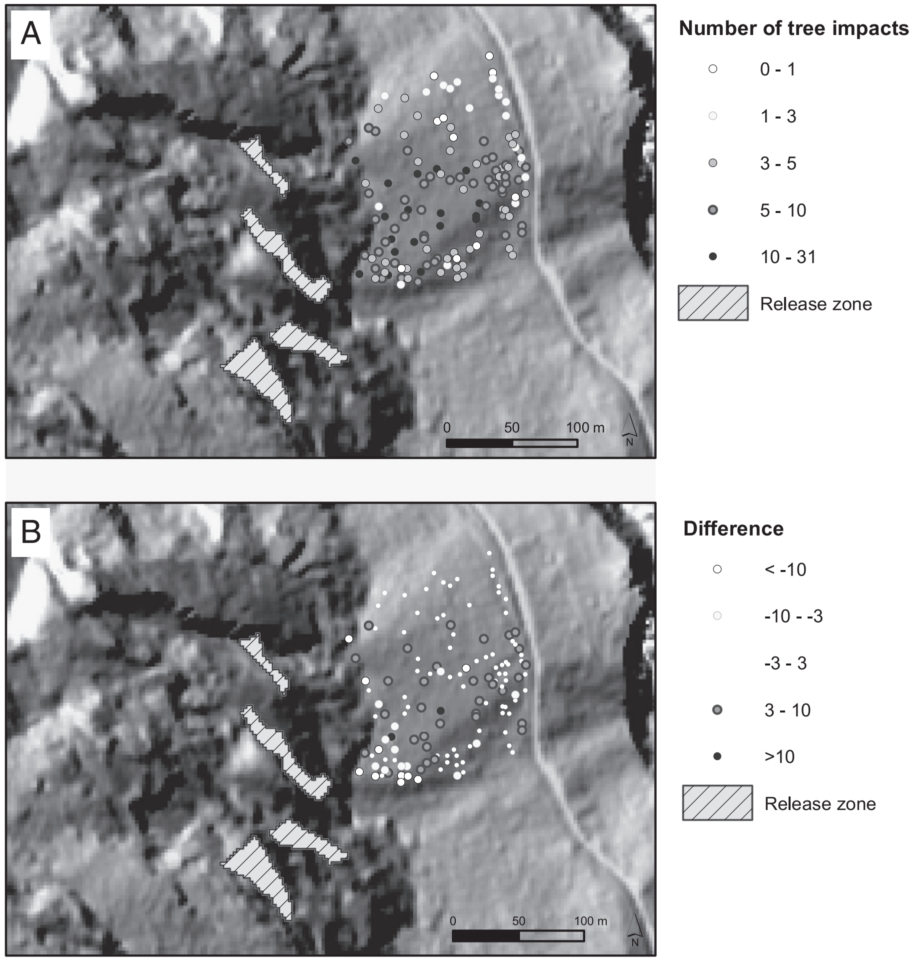

Fig. 8. (A) Spatial distribution of the normalized number of tree impacts computed with simulation S3 (i.e. active rockfall slopes determined from geomorphic and geologic maps) and (B) differences between simulated and observed number of rock impacts on trees.

downslope (Kirkby and Statham, 1975; Erismann and Abele, 2001; Meissl, 2001; Dorren, 2003) and where they are therefore concentrated at, or even deposited beyond, the base of the slope.

The combination of ecological sources of information with the 3D modeling approach also allowed translation of simulated (relative) frequencies of block propagations into "real" (or, at least, realistic) return periods of rockfall events. This translation is of particular relevance for hazard assessments and related land-use planning measures for which both data on intensity (i.e., kinetic energy) a n d probability of occurrence (i.e., return period) are key prerequisistes (Raetzo et al., 2002).

5.2. Main limitations of the approach

While the comparison of observed and modeled rockfall frequencies yielded very satisfactory results overall, we realize that the correspondence between the predicted and the observed number of tree hits (or GD) remained quite poor in several sectors of the study slope and irrespective of the approaches (source cells, block sizes) used. First of all, and as stochastic elements are involved in rockfall processes, a complete agreement of observed and simulated rockfalls is unlikely to occur. In addition, the reasons for the discrepancies between the model and observations also have to be accounted for to different sources of errors. A first factor which might have affected the MAE could stem from the nature of the dendrogeomorphic dataset. The spatial distribution of rockfalls based on dendrogeomorphic information relies on 737 GD observed in 133 trees impacted over the past 127 yr. Possibly, this dataset, although unusually large for a rockfall slope, may not represent the full distribution of rockfalls and trajectories that is obtained from a very large number (e.g., release of 395,700 rocks and 26,479 tree impacts in S1) of simulations (Bourrier et al., 2009).

Interestingly, we also observe that the average number of rock impacts per tree was higher in reality than simulated by RockyFor3D in the south-westernmost segment of the slope (19 trees) where a large (80 m^3) rockfall occurred in November 2002. In this particular case, the underestimation of real activity by the model (representing 30% of the total MAE in S8), is probably related to its parameterization. Indeed, RockyFor3D simulates individual rockfalls (Dorren et al., 2006) and does not therefore take account of the interaction of fragments as observed in falling rock masses. In addition, it is likely that multiple scars have been inflicted to several trees by the same event which could have led to a further overestimation of activity in this portion of the site. Moreover, complex phenomena such as the fragmentation of rocks after impacts are currently not reproduced by rockfall simulation models (Crosta and Agliardi, 2004; Volkwein et al., 2011), although these processes have been demonstrated to create multiple scars on individual stems or individual scars on several trees (Trappmann and Stoffel, 2013).

Finally, part of the difference between the predicted and the observed number of tree hits also stems from the fact that the presence of rockfall nets cannot be considered in the rockfall code. As a result,

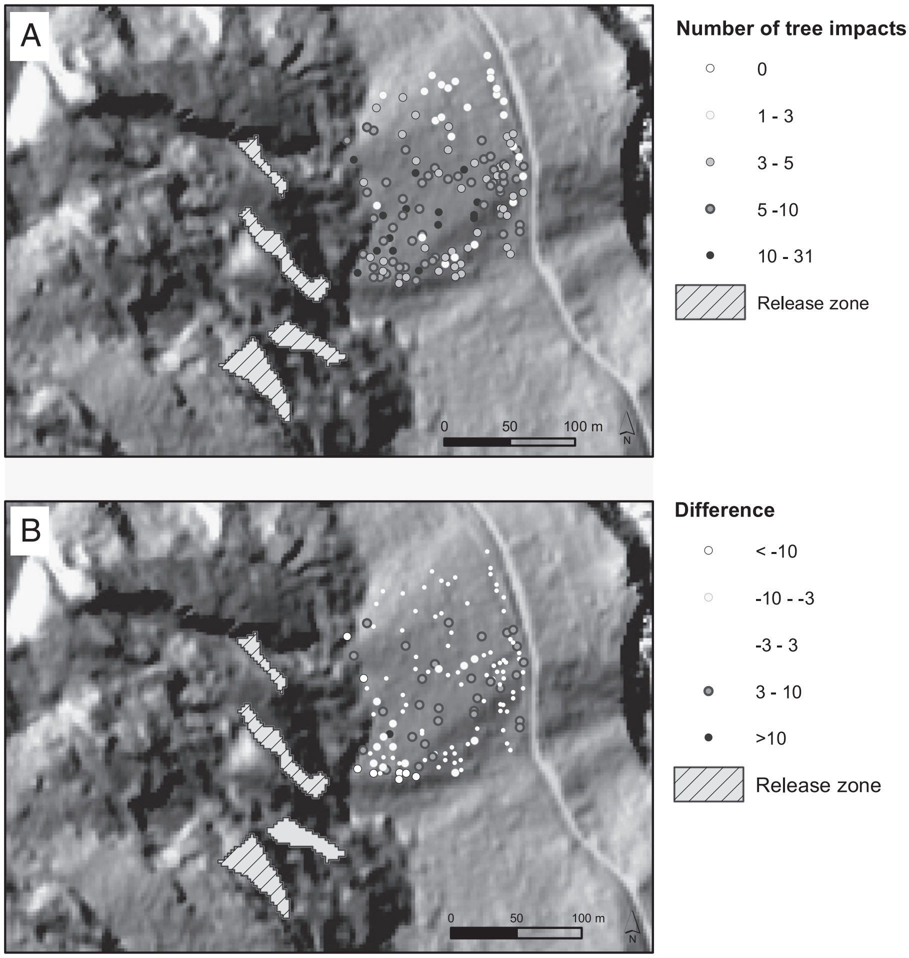

Fig. 9. (A) Spatial distribution of the normalized number of tree impacts computed with composite simulation S8 (i.e. weighted mean of simulations S4–S7) and (B) differences between simulated and observed number of rock impacts on trees.

this may have led to an overestimation of recent activity below the nets in the simulation runs.

6. Conclusion

This study addresses interactions between biotic (tree growth) and abiotic (rockfalls) processes to improve and complement our understanding of tree–rock interactions. Through the use of dendrogeomorphic and 3D rockfall simulation modeling approaches on a forested slope in the Swiss Alps, we demonstrate that differences between the simulated and the observed frequencies of rockfalls can be minimized through a precise definition of active source areas and a realistic relative distribution of block sizes as observed in the field. Through the use of systematic iterative processes based on the aggregation and disaggregation of release zones and the systematic assessment of model accuracy through the comparison of model outputs with data from tree-ring analyses, we were able to demonstrate that the delineation of optimal source areas of rockfalls can be improved considerably.

The convergence of dendrogeomorphic and modeling approaches also permitted the transformation highly statistically significant values for rockfall frequencies obtained from the RockyFor3D model into real frequencies. By following the proposed approach, hazard mapping will be greatly improved as it allows a reliable spatial characterization of rockfall frequencies in terms of return intervals. In areas where hazard mapping is required for land-use planning purposes (e.g., Raetzo et al., 2002; Jaboyedoff et al., 2005), a combination of ecological and modeling approaches should be used systematically wherever woody vegetation is available so as to increase the accuracy of modeling outputs and hence to improve hazard assessments.

Acknowledgment

The authors acknowledge financial support from the community of Eisten and the canton of Valais.

References

Bannan, M.W., 1936. Vertical resin ducts in the secondary wood of the *Abietineae*. New Phytologist 35, 11–46.
Bearth, P., 1978. Geologischer Atlas der Schweiz, Blatt 1308 St. Niklaus, 1:25000. Birkhäuser: Basel.
Bollschweiler, M., Stoffel, M., Schneuwly, D.M., 2008. Dynamics in debris-flow activity on a forested cone — a case study using different dendroecological approaches. Catena 72, 67–78.
Bourrier, F., Dorren, L., Nicot, F., Berger, F., Darve, F., 2009. Toward objective rockfall trajectory simulation using a stochastic impact model. Geomorphology 110, 68–79.
Brauner, M., Weinmeister, W., Agner, P., Vospernik, S., Hoesle, B., 2005. Forest management decision support for evaluating forest protection effects against rockfall. Forest Ecology and Management 207, 75–85.
Ciabocco, G., Boccia, L., Ripa, M.N., 2009. Energy dissipation of rockfalls by coppice structures. Natural Hazards and Earth System Sciences 9, 993–1001.
Crosta, G.B., Agliardi, F., 2004. Parametric evaluation of 3D dispersion of rockfall trajectories. Natural Hazards and Earth System Sciences 4, 583–598.
Dorren, L.K.A., 2003. A review of rockfall mechanics and modelling approaches. Progress in Physical Geography 27, 69–87.
Dorren, L.K.A., 2012. Rockyfor3D (v5.0) revealed — transparent description of the complete 3D rockfall model. ecorisQ paper. (www.ecorisq.org, 31 pp.).
Dorren, L.K.A., Berger, F., 2006. Stem breakage of trees and energy dissipation at rockfall impacts. Tree Physiology 26, 63–71.

Dorren, L.K.A., Berger, F., Le Hir, C., Mermin, E., Tardif, P., 2005. Mechanisms, effects and management implications of rockfall in forests. Forest Ecology and Management 215, 183–195.

Dorren, L.K.A., Berger, F., Putters, U.S., 2006. Real size experiments and 3D simulation of rockfall on forested and non-forested slopes. Natural Hazards and Earth System Sciences 6, 145–153.

Dorren, L.K.A., Berger, F., Jonsson, M., Krautblatter, M., Mölk, M., Stoffel, M., Wehrli, A., 2007. State of the art in rockfall–forest interactions. Schweizerische Zeitschrift für Forstwesen 158, 128–141.

Douglas, G.R., 1980. Magnitude frequency study of rockfall in Co.Antrim, N. Ireland. Earth Surface Processes and Landforms 5, 123–129.

Dussauge-Peisser, C., Helmstetter, A., Grasso, J.-R., Hantz, D., Desvarreux, P., Jeannin, M., Giraud, A., 2002. Probabilistic approach to rock fall hazard assessment: potential of historical data analysis. Natural Hazards and Earth System Sciences 2, 15–26.

Erismann, T.H., Abele, G., 2001. Dynamics of Rockslides and Rockfalls. Springer-Verlag, Berlin (316 pp.).

Gardner, J.S., 1980. Frequency, magnitude, and spatial distribution of mountain rockfalls and rockslides in the Highwood Pass Area, Alberta, Canada. In: Coates, R., Vitek, J. (Eds.), Thresholds in Geomorphology. Allen and Unwin, New York, pp. 267–295.

Grime, J.P., 2001. Plant Strategies, Vegetation Processes, and Ecosystem Properties. Wiley, Chichester (417 pp.).

Gsteiger, P., 1993. Steinschlagschutzwald — Ein Beitrag zur Abgrenzung, Beurteilung und Bewirtschaftung. Schweizerische Zeitschrift für Forstwesen 144, 115–132.

Gunderson, L.H., 2000. Ecological resilience—in theory and applications. Annual Review of Evolution Ecology, and Systematics 31, 425–439.

Hantz, D., Vengeon, J.M., Dussauge-Peisser, C., 2003. An historical, geomechanical and probabilistic approach to rock-fall hazard assessment. Natural Hazards and Earth System Sciences 3, 693–701.

Jaboyedoff, M., Dudt, J.P., Labiouse, V., 2005. An attempt to refine rockfall zoning based on kinetic energy, frequency and fragmentation degree. Natural Hazards and Earth System Sciences 5, 621–632.

Kirkby, M.J., Statham, I., 1975. Surface stone movement and scree formation. Journal of Geology 83, 349–362.

Lewis, P.A.W., Orav, E.J., 1989. Simulation Methodology for Statisticians, Operations Analysts, and Engineers, vol. 1. Wadsworth & Brooks/Cole (375 pp.).

Loye, A., Jaboyedoff, M., Pedrazzini, A., 2009. Identification of potential rockfall source areas at a regional scale using a DEM based geomorphometric analysis. Natural Hazards and Earth System Sciences 9, 1643–1653.

Luckman, B.H., 1976. Rockfalls and rockfall inventory data; some observations from the Surprise Valley, Jasper National Park, Canada. Earth Surface Processes 1, 287–298.

Lundström, T., Jonas, T., Stöckli, V., Ammann, W., 2007. Anchorage of mature conifers: resistive turning moment, root–soil plate geometry and root growth orientation. Tree Physiology 27, 1217–1227.

Lundström, T., Jonsson, M.J., Volkwein, A., Stoffel, M., 2009. Reactions and energy absorption of trees subject to rockfall: a detailed assessment using a new experimental method. Tree Physiology 29, 345–359.

Marston, R.A., 2010. Geomorphology and vegetation on hillslopes: interactions, dependencies, and feedback loops. Geomorphology 116, 206–217.

Matsuoka, N., Sakai, H., 1999. Rockfall activity from an alpine cliff during thawing periods. Geomorphology 28, 309–328.

Meissl, G., 1998. Modellierung der Reichweite von Felsstürzen. Fallbeispeile zur GISgestützten Gefahrenbeurteilung aus dem Beierischen und Tiroler Alpenraum. Innsbrucker Geografische Studien 28. Ph.D. Thesis, Universität Innsbruck, Innsbruck; (249 pp.).

Meissl, G., 2001. Modelling the runout distances of rockfalls using a geographic information system. Zeitschrift für Geomorphologie 125, 129–137.

Mowrer, H.T., 1997. Propagating uncertainty through spatial estimation processes for old-growth subalpine forests using sequential Gaussian simulation in GIS. Ecological Modelling 98, 73–86.

Moya, J., Corominas, J., Pérez Arcas, J., Baeza, C., 2010. Tree-ring based assessment of rockfall frequency on talus slopes at Solà d'Andorra, Eastern Pyrenees. Geomorphology 118, 393–408.

Perret, S., Stoffel, M., Kienholz, H., 2006. Spatial and temporal rockfall activity in a forest stand in the Swiss Prealps – a dendrogeomorphological case study. Geomorphology 74, 219–231.

Pfeiffer, T.J., 1989. Rockfall Hazard Analysis using Computer Simulation of Rockfalls, Master of Science Thesis. Colorado School of Mines.

Porter, S.C., Orombelli, G., 1981. Alpine rockfall hazards. American Scientist 69, 67–75.

Raetzo, H., Lateltin, O., Bollinger, D., Tripet, J.P., 2002. Hazard assessment in Switzerland — codes of practice for mass movements. Bulletin of Engineering Geology and the Environment 61, 263–268.

Rixen, C., Haag, S., Kulakowski, D., Bebi, P., 2007. Natural avalanche disturbance shapes plant diversity and species composition in subalpine forest belt. Journal of Vegetation Science 18, 735–742.

Schneuwly, D.M., 2009. Tree rings and rockfall – Anatomic tree reactions and spatio-temporal rockfall analysis. PhD Thesis, Department of Geosciences, Geography, University of Fribourg, Switzerland; (160 pp.).

Schneuwly, D.M., Stoffel, M., Dorren, L.K.A., Berger, F., 2009. Three-dimensional analysis of the anatomical growth response of European conifers to mechanical disturbance. Tree Physiology 29, 1247–1257.

Seidl, R., Fernandes, P.M., Fonseca, T.F., Gillet, F., Jönsson, A.M., Merganicova, K., Netherer, S., Arpaci, A., Bontemps, J.D., Bugmann, H., Gonzalez-Olabarria, J.R., Lasch, P., Meredieu, C., Moreira, F., Schelhaas, M.J., Mohren, F., 2011. Modelling natural disturbances in forest ecosystems: a review. Ecological Modelling 222, 903–924.

Šilhán, K., Brázdil, R., Pánek, T., Dobrovolný, P., Kašičková, L., Tolasz, R., Turský, O., Václavek, M., 2011. Evaluation of meteorological controls of reconstructed rockfall activity in the Czech Flysch Carpathians. Earth Surface Processes and Landforms 36, 1898–1909.

Stoffel, M., 2006. A review of studies dealing with tree rings and rockfall activity: the role of dendrogeomorphology in natural hazard research? Natural Hazards 39, 51–70.

Stoffel, M., 2008. Dating past geomorphic processes with tangential rows of traumatic resin ducts. Dendrochronologia 26, 53–60.

Stoffel, M., Bollschweiler, M., 2008. Tree-ring analysis in natural hazards research — an overview. Natural Hazards and Earth System Science 8, 187–202.

Stoffel, M., Hitz, O.M., 2008. Snow avalanche and rockfall impacts leave different anatomical signatures in tree rings of *Larix decidua*. Tree Physiology 28, 1713–1720.

Stoffel, M., Perret, S., 2006. Reconstructing past rockfall activity with tree rings: some methodological considerations. Dendrochronologia 24, 1–15.

Stoffel, M., Lièvre, I., Monbaron, M., Perret, S., 2005a. Seasonal timing of rockfall activity on a forested slope at Täschgufer (Valais, Swiss Alps) — a dendrochronological approach. Zeitschrift für Geomorphologie 49, 89–106.

Stoffel, M., Schneuwly, D., Bollschweiler, M., Lièvre, I., Delaloye, R., Myint, M., Monbaron, M., 2005b. Analyzing rockfall activity (1600–2002) in a protection forest — a case study using dendrogeomorphology. Geomorphology 68, 224–241.

Stoffel, M., Bollschweiler, M., Butler, D.R., Luckman, B.H., 2010. Tree Rings and Natural Hazards. A State-of-the-Art. Springer, Heidelberg, Berlin, New-York (505 pp.).

Stokes, A., 2006. Selecting tree species for use in rockfall-protection forests. Forest Snow and Landscape Research 80, 77–86.

Stokes, A., Salin, F., Kokutse, A.D., Berthier, S., Jeannin, H., Mochan, S., Dorren, L., Kokutse, N., Ghani, M.A., Fourcaud, T., 2005. Mechanical resistance of different tree species to rockfall in the French Alps. Plant and Soil 278, 107–117.

Toppe, R., 1987. Terrain models — a tool for natural hazard mapping. In Salm, B. and Gubler, H. (Eds.), avalanche formation, movement and effects. International Association of Hydrological Sciences 162, 629–638.

Trappmann, D., Stoffel, M., 2013. Counting scars on tree stems to assess rockfall hazards: A low effort approach, but how reliable? Geomorphology 181, 180–186.

Van Dijke, J.J., van Westen, C.J., 1990. Rockfall hazard: a geomorphological application of neighbourhood analysis with ILWIS. ITC Journal 1, 40–44.

Veblen, T., Hadley, K., Nel, E., Kitzberger, M., Villalba, R., 1994. Disturbance regime and disturbance interactions in a Rocky Mountain subalpine forest. Journal of Ecology 82, 125–135.

Volkwein, A., Schellenberg, K., Labiouse, V., Agliardi, F., Berger, F., Bourrier, F., Dorren, L.K.A., Gerber, W., Jaboyedoff, M., 2011. Rockfall characterisation and structural protection — a review. Natural Hazards and Earth System Sciences 11, 2617–2651.

White, P.S., Jentsch, A., 2001. The search for generality in studies of disturbance and ecosystem dynamics. Progress in Botany 62, 399–449.

White, P.S., Pickett, S.T.A., 1985. Natural disturbances and patch dynamics: an introduction. In: White, P.S., Pickett, S.T.A. (Eds.), The Ecology of Natural Disturbances and Patch Dynamics. Academic Press, San Diego, pp. 1–15.